Editors' Suggestion

Absolute Negative Mobility of an Active Tracer in a Crowded Environment

Pierre Rizkallah,[1] Alessandro Sarracino,[2,3] Olivier Bénichou,[4] and Pierre Illien[1]
[1]*Sorbonne Université, CNRS, Laboratoire de Physico-Chimie des Électrolytes et Nanosystèmes Interfaciaux (PHENIX), 4 Place Jussieu, 75005 Paris, France*
[2]*Dipartimento di Ingegneria, Università della Campania Luigi Vanvitelli, 81031 Aversa (CE), Italy*
[3]*Istituto dei Sistemi Complessi—CNR, P.le Aldo Moro 2, 00185, Rome, Italy*
[4]*Sorbonne Université, CNRS, Laboratoire de Physique Théorique de la Matière Condensée (LPTMC), 4 Place Jussieu, 75005 Paris, France*

(Received 2 December 2022; revised 17 February 2023; accepted 11 April 2023; published 22 May 2023)

Absolute negative mobility (ANM) refers to the situation where the average velocity of a driven tracer is opposite to the direction of the driving force. This effect was evidenced in different models of nonequilibrium transport in complex environments, whose description remains effective. Here, we provide a microscopic theory for this phenomenon. We show that it emerges in the model of an active tracer particle submitted to an external force and which evolves on a discrete lattice populated with mobile passive crowders. Resorting to a decoupling approximation, we compute analytically the velocity of the tracer particle as a function of the different parameters of the system and confront our results to numerical simulations. We determine the range of parameters where ANM can be observed, characterize the response of the environment to the displacement of the tracer, and clarify the mechanism underlying ANM and its relationship with negative differential mobility (another hallmark of driven systems far from the linear response).

DOI: 10.1103/PhysRevLett.130.218201

Introduction.—Predicting the response of a tracer particle submitted to an external driving and evolving in a complex environment is a central challenge in statistical physics [1,2]. The relation between the force applied to the tracer and its velocity can display a number of striking anomalies, in particular, when the tracer evolves very far from equilibrium. One of the most intriguing behaviors is the onset of an inverse current, which is opposite to the driving force and which was evidenced, for instance, in the very simple setting of a Brownian particle forced in a periodically modulated potential [3]. In the specific context of particle transport, this effect is known as absolute negative mobility (ANM).

This intriguing effect actually finds important applications in sorting micrometric particles. Relying on this counterintuitive response, microfluidic chips that allow efficient separations of particles have been successfully designed [4–6], and recent developments may even allow tunable mass separation [7]. At the theoretical level, understanding ANM is a challenge. Indeed, this effect emerges from the interactions between the tracer and its environment, which needs to be modulated in space and/or in time for ANM to emerge. This has motivated a whole field of research in the past, and different ways to model such an environment have been explored so far: through an effective persistence of the tracer [8], periodic ratchets [3,9–11], effective tracer-bath interactions [12], coupled thermodynamic forces [13], or steady and periodic velocity fields [14–16]. However, the case of an environment made of mobile crowders (and the possibility for ANM to emerge in such a setting) has not been addressed, in spite of its importance in the modeling of transport in biological context, for instance. This is a particularly difficult theoretical problem, since it requires the treatment of a many-body problem.

Our model, which tackles this issue, considers an active tracer particle submitted to an external force, which evolves in a dynamical environment of mobile hardcore crowders on a lattice, whose dynamics is accounted for explicitly. This model thus belongs to the important class of exclusion processes, which are paradigmatic models of nonequilibrium statistical physics and which received considerable attention, both in 1D [17,18] and in higher dimensions [19–26]. On top of providing an explicit description of the environment of the tracer, which allows us to characterize the response of the environment to the displacement of the tracer, this model is analytically tractable, gives accurate results in a wide range of parameters, and elucidates the conditions under which ANM is observed. We also present a qualitative argument valid at low density, which explains the main phenomenon in terms of the relevant characteristic timescales. In particular, we show how ANM emerges from the trapping of the tracer particle by the passive crowders. Finally, our approach clarifies the relationship between ANM and negative differential mobility (another hallmark of driven systems far from the linear response).

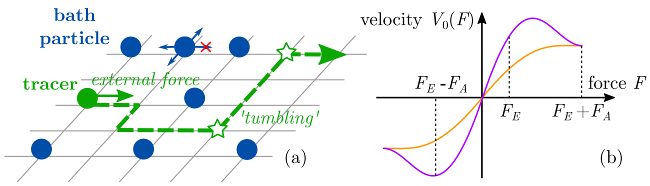

FIG. 1. (a) Sketch of the system under study: a tracer particle (in green), which is active and submitted to an external driving, evolves in a bath of passive crowders. (b) Typical force-velocity curve of a passive tracer with and without negative differential mobility (in purple and orange, respectively).

Model.—We consider a d-dimensional cubic lattice ($d \geq 2$) of unit spacing, with base vectors $\boldsymbol{e}_1, \ldots, \boldsymbol{e}_d$ (we use the convention $\boldsymbol{e}_{-\mu} = -\boldsymbol{e}_\mu$). The bath particles perform continuous-time symmetric random walks: at times drawn randomly from an exponential clock of average τ^*, they pick one of their $2d$ neighboring sites at random and jump onto if it is free (otherwise, the jump is not performed). The tracer particle also performs jumps onto neighboring sites, but is under the influence of two forces: (i) a constant external force, pointing in direction $\boldsymbol{e}_1$, and of intensity F_E and (ii) an active force of intensity F_A and whose direction $\boldsymbol{e}_\chi$ ($\chi \in \{\pm 1, \ldots, \pm d\}$) changes randomly at exponentially distributed times of average τ_α. This active force represents the "propulsion" of the particle (for instance, that of a microswimmer, such as a bacteria or an active colloid), whereas the force F_E represents some external driving imposed on the active particle that may originate from a solvent flow or a magnetic field, for instance [see Fig. 1(a) for a sketch of the model]. The tracer jumps in direction $\boldsymbol{e}_\mu$ if the target site is empty, with rate $p_\mu^{(\chi)}/\tau$, where $p_\mu^{(\chi)} = \{\exp[(F_A \boldsymbol{e}_\chi + F_E \boldsymbol{e}_1) \cdot \boldsymbol{e}_\mu / 2]/Z\}$. The normalization factor Z is such that $\sum_\mu p_\mu^{(\chi)} = 1$ (we use the shorthand notation $\sum_\mu \equiv \sum_{\mu \in \{\pm 1, \ldots, \pm d\}}$). The characteristic jump time of the tracer τ will be taken as the unit time of the model. Finally, the hardcore interactions between the particles are enforced by the condition that there can only be one particle per site. The position of the tracer at time t is denoted by $\boldsymbol{X}_t$, and we will be interested in its projection along the direction of the external force $X_t \equiv \boldsymbol{X}_t \cdot \boldsymbol{e}_1$. The velocity reached by the tracer (along direction 1) in the stationary state will be denoted by $V \equiv \lim_{t \to \infty}(d\langle X_t \rangle / dt)$.

Simple argument for ANM.—Before going into the details of our analytical derivation, we present a simple argument to explain the emergence of ANM in the model described above and its relation to negative differential mobility (NDM). The latter refers to the situation where a particle submitted to a constant external force F_E may display a velocity that decreases with the intensity of the force while remaining positive [22,26–33]. This effect typically originates from the trapping effects induced by the environment of the tracer when the former is not mobile enough (see below for a description of this mechanism) [28].

For illustration, we consider the simple situation where the tracer is submitted to an active force F_A that may only point in directions $\pm \boldsymbol{e}_1$. In the limit where the persistence time is greater than other timescales, the average velocity of the tracer can therefore be estimated as the average of the velocities conditioned on these two states $V \simeq \frac{1}{2}[V_0(F_E + F_A) + V_0(F_E - F_A)]$, where $V_0(F)$ is the stationary velocity of a passive particle (i.e., with $F_A = 0$ and/or $\tau_\alpha = 0$) submitted to an external force F. We assume that $F_E > 0$, and we first consider the case where the tracer does not display negative differential mobility. Its velocity is then a monotonic function of the force undergone by the tracer [see Fig. 1(b) for a sketched representation of the force-velocity curves]. In this situation, it is clear that V will be of the sign of F_E, and no absolute negative mobility can be observed. However, when the tracer displays negative differential mobility, one may observe the situation where $|V_0(F_E - F_A)| > |V_0(F_E + F_A)|$, therefore resulting in a situation where average velocity V is negative although $F_E > 0$.

These simple considerations clarify the relationship between ANM and NDM. To summarize, the velocity of the active tracer can be understood as an average over the velocities conditioned over the different possible orientations of the active force. If this conditional velocity is a nonmonotonic function of the force (NDM), the average velocity can become negative (ANM).

Results.—We now turn to the details of our analytical approach. We define $P_\chi(\boldsymbol{R}, \eta; t)$ as the probability that the tracer is at position $\boldsymbol{R}$, the active force in direction $\boldsymbol{e}_\chi$, and the environment in configuration $\eta = (\eta_{\boldsymbol{r}})_{\boldsymbol{r} \in \boldsymbol{Z}^d}$ (where $\eta_{\boldsymbol{r}}$ is a random variable equal to 1 if there is a bath particle on the site $\boldsymbol{r}$ and 0 otherwise) at time t. This quantity obeys the following master equation:

$$2d\tau^* \partial_t P_\chi(\boldsymbol{R}, \eta; t) = \mathcal{L}_\chi P_\chi - \alpha P_\chi + \frac{\alpha}{2d-1} \sum_{\chi' \neq \chi} P_{\chi'}, \quad (1)$$

where $\alpha = 2d\tau^*/\tau_\alpha$ is a dimensionless rate of reorientation of the active force, and $\mathcal{L}_\chi$ is the evolution operator when the active force is in direction $\boldsymbol{e}_\chi$,

$$\mathcal{L}_\chi P_\chi = \sum_{\nu=1}^{d} \sum_{\boldsymbol{r} \neq \boldsymbol{R} - \boldsymbol{e}_\nu, \boldsymbol{R}} [P_\chi(\boldsymbol{R}, \eta^{\boldsymbol{r},\nu}; t) - P_\chi(\boldsymbol{R}, \eta; t)] + \frac{2d\tau^*}{\tau} \sum_\mu p_\mu^{(\chi)} [(1 - \eta_{\boldsymbol{R}}) P_\chi(\boldsymbol{R} - \boldsymbol{e}_\mu, \eta; t) - (1 - \eta_{\boldsymbol{R}+\boldsymbol{e}_\mu}) P_\chi(\boldsymbol{R}, \eta; t)]. \quad (2)$$

We denote by $\eta^{\boldsymbol{r},\nu}$ the configuration obtained from η by switching the occupations of sites $\boldsymbol{r}$ and $\boldsymbol{r} + \boldsymbol{e}_\nu$. The first term in Eq. (2) accounts for the jumps performed by bath particles, whereas the second term accounts for the jumps performed by the tracer.

From Eq. (1), we derive the expression of the average velocity by multiplying Eq. (1) by X_t and averaging over all positions $\boldsymbol{R}$ and lattice configurations η (see Supplemental Material for details on analytical calculations [34]),

$$\frac{d\langle X_t\rangle}{dt} = \frac{1}{2d\tau}\sum_{\chi}\{p_1^{(\chi)}[1-k_{\boldsymbol{e}_1}^{(\chi)}] - p_{-1}^{(\chi)}[1-k_{\boldsymbol{e}_{-1}}^{(\chi)}]\}, \quad (3)$$

where $k_{\boldsymbol{r}}^{(\chi)} = \langle \eta_{X_t+\boldsymbol{r}}\rangle_\chi = 2d\sum_{\boldsymbol{R},\eta}\eta_{\boldsymbol{R}+\boldsymbol{r}}P_\chi(\boldsymbol{R},\eta;t)$ is the average occupation of position $\boldsymbol{r}$ in the frame of reference of the tracer, conditioned on the active force being in direction $\boldsymbol{e}_\chi$. These quantities obey the following equation, obtained by multiplying Eq. (1) by $\eta_{X_t+\boldsymbol{r}}$ and summing over all tracer positions and lattice configurations:

$$2d\tau^*\partial_t k_{\boldsymbol{r}}^{(\chi)} = \sum_\mu (\nabla_\mu - \delta_{\boldsymbol{r},\boldsymbol{e}_\mu}\nabla_{-\mu})k_{\boldsymbol{r}}^{(\chi)} + \frac{\alpha}{2d-1}\sum_{\chi'\neq\chi}k_{\boldsymbol{r}}^{(\chi')} - \alpha k_{\boldsymbol{r}}^{(\chi)} + \frac{2d\tau^*}{\tau}\sum_\mu p_\mu^{(\chi)}\langle(1-\eta_{X_t+\boldsymbol{e}_\mu})\nabla_\mu\eta_{X_t+\boldsymbol{r}}\rangle_\chi, \quad (4)$$

where $\nabla_\mu k_{\boldsymbol{r}}^{(\chi)} = k_{\boldsymbol{r}+\boldsymbol{e}_\mu}^{(\chi)} - k_{\boldsymbol{r}}^{(\chi)}$ is a discrete gradient operator.

The evolution equation for the density profiles $k_{\boldsymbol{r}}^{(\chi)}$ is not closed because it involves the correlation functions $\langle\eta_{X_t+\boldsymbol{e}_\mu}\eta_{X_t+\boldsymbol{r}}\rangle_\chi$. Obtaining an evolution equation for these correlation functions would actually involve correlation functions of higher order, and so on. We then resort to a decoupling approximation [28,35,36], which consists in neglecting second order fluctuations around the mean, implying $\langle\eta_{X_t+\boldsymbol{e}_\mu}\eta_{X_t+\boldsymbol{r}}\rangle_\chi \simeq k_{\boldsymbol{e}_\mu}^{(\chi)}k_{\boldsymbol{r}}^{(\chi)}$. This approximation is inspired by our previous work on the case of a passive tracer submitted to a constant external force ($F_A = 0$ and $F_E \neq 0$) [35]. We recently adapted this approximation scheme to study the case of an active tracer with no external force ($F_A \neq 0$ and $F_E = 0$) [36]. The present work goes beyond both these studies, as it addresses the situation where both the external force and the active force are present. From a technical point of view, this increases the complexity of the analytical approach, since we now lack most of the symmetries that used to facilitate our derivation. From a physical point of view, it reveals a new striking phenomenon, namely ANM.

This approximation enables us to close Eq. (4) and to obtain the following set of equations obeyed by the density profiles $k_{\boldsymbol{r}}$:

$$2d\tau^*\partial_t k_{\boldsymbol{r}}^{(\chi)} = \sum_\mu A_\mu^{(\chi)}(\nabla_\mu + \delta_{\boldsymbol{r},\boldsymbol{e}_\mu})k_{\boldsymbol{r}} - \alpha k_{\boldsymbol{r}}^{(\chi)} + \frac{\alpha}{2d-1}\sum_{\chi'\neq\chi}k_{\boldsymbol{r}}^{(\chi')}. \quad (5)$$

We denoted $A_\mu^{(\chi)} \equiv 1 + (2d\tau^*/\tau)p_\mu^{(\chi)}[1-k_{\boldsymbol{e}_\mu}^{(\chi)}]$ and adopted the convention $k_{\boldsymbol{0}}^{(\chi)} = 0$. Note that this decoupling approximation preserves the spatial dependencies of the density profiles and goes beyond trivial mean field, which would consist in writing $\langle\eta_{\boldsymbol{r}}\rangle = \rho$ for any $\boldsymbol{r}$.

We provide in the Supplemental Material [34] the stationary solution of Eq. (5), which allows us to write explicitly the density profiles $k_{\boldsymbol{r}}$ in terms of their values at the sites in the vicinity of the tracer $k_{\boldsymbol{e}_\nu}$. In turn, these values are shown to satisfy a closed system of equations. This finally provides the analytical solution of the stationary profiles (up to the numerical solution of this implicit system of equations) and of the stationary velocity [Eq. (3)]. For a given value of the density, when the active force F_A and the characteristic jump time of the bath particles τ^* are small enough compared to that of the tracer τ, the average velocity of the tracer remains positive at all values of the external force F_E. However, we observe that, for a sufficiently large persistence time τ_α, when the active force is large enough or when the bath particles are sufficiently slow compared to the tracer ($\tau^* \gg \tau$), the velocity can become a negative function of the external force [Fig. 2(a)], which is the signature of ANM. We compare the value of the velocity predicted by our analytical theory with results from Monte Carlo simulations of the microscopic dynamics and observe an excellent agreement, which confirms the relevance of our decoupling approximation to study the dynamics of an active, driven tracer. As a comparison with our previous work, we emphasize that the decoupling approximation was even more accurate when it was applied to calculate the diffusion coefficient of a tracer with $F_E = 0$ [36].

Interestingly, we also show in the Supplemental Material [34] that our approach also provides an analytical expression for the generalized Einstein relation [14,37] that is derived explicitly from microscopic considerations. Finally, our analytical framework, which fully accounts for the microscopic details of the environment of the tracer, allows us to quantify the perturbation induced by its displacement. Indeed, as a by-product of our calculation, we compute

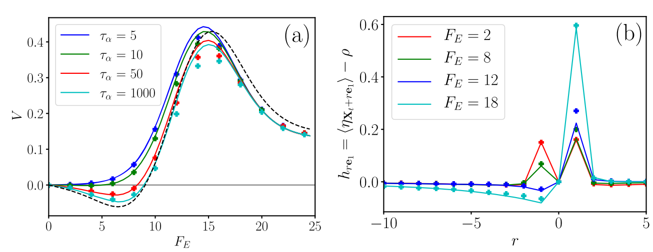

FIG. 2. (a) Stationary velocity of the tracer particle along the direction of the external force F_E on a 2D lattice. Lines: decoupling approximation [Eqs. (3) and (5)]; symbols: Monte Carlo simulations [34]; dashed line: qualitative argument in the limit of infinite persistence [Eq. (7) for $\tau_\alpha = \infty$]. (b) Density profiles (relative to the reference value ρ) along the direction of F_E in the frame of reference of the tracer, as a function of the distance to the tracer r [here $\tau_\alpha = 50$, corresponding to the red line of (a)]. In both plots, the parameters are $\rho = 0.1$, $\tau^* = 30$, $\tau = 1$, $F_A = 12$.

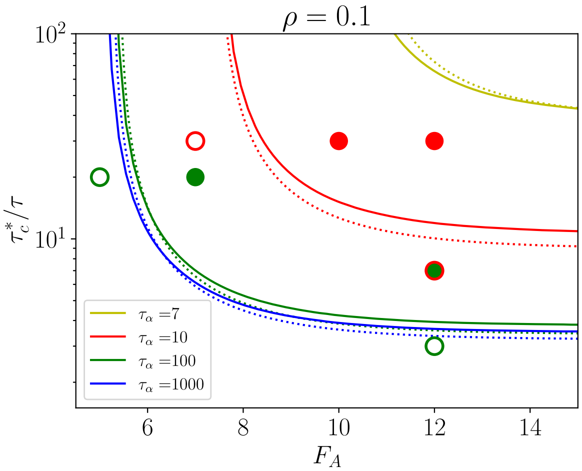

FIG. 3. Phase diagram for ANM. Above the lines, the theory predicts absolute negative mobility. Solid lines: decoupling approximation [Eqs. (3) and (5)]. Dotted lines: critical value τ_c^*/τ determined from the low-density qualitative argument [Eq. (7)]. Symbols: Monte Carlo simulations; a filled circle means ANM is observed, an empty one means it is not.

from Eq. (5) the density profiles in the reference frame of the tracer. Their typical spatial dependence is plotted in Fig. 2(b). It shows that ANM has a signature on the response of the environment, and that a small density excess may develop behind the tracer ($r < 0$) when its average velocity becomes negative.

Phase diagram.—Relying on our analytical approach, we can explore a wide range of parameters to determine domains of existence of ANM. According to our previous studies on NDM [28,30], for an infinitely persistent tracer (in the present formalism, this corresponds to $F_A = 0$ and $F_E > 0$), this phenomenon occurs when, for a given value of the density, the ratio between the jump time of the obstacles and that of the tracer τ^*/τ is sufficiently large. Here, the emergence of ANM is also determined by the parameters that control the activity of the tracer (the magnitude of the active force F_A and the average persistence time of its orientation τ_α). In Fig. 3, we show the critical value of the characteristic jump time of bath particles τ_c^* (rescaled by τ) above which ANM occurs, as a function of the active force F_A for different values of the persistence time τ_α and for a fixed value of the density of crowders ρ, and confront our analytical predictions to results from numerical simulations. Details on the procedure to construct this plot are given in the Supplemental Material [34].

This phase diagram gives an insight on the range of parameters where ANM can be observed. For instance, for $F_A \simeq 10$ and $\tau^*/\tau \simeq 10$, it shows that ANM is observed as soon as τ_α reaches a critical value comprised between 10 and 100. In order to relate these values to more realistic systems, we can compute a Péclet number for the active tracer as $\mathrm{Pe} \sim v_0/\sqrt{D_T D_R}$, where v_0 is the typical propulsion velocity, and D_T (respectively, $D_R \sim \tau_\alpha^{-1}$) is the translational (respectively, rotational) diffusion coefficient of the active particle. In our system of units, $D_T = 1$ and $v_0 \simeq 1$ (when F_A is large enough), so that we simply get $\mathrm{Pe} \sim \sqrt{\tau_\alpha}$. In the example above, the condition for ANM to be observed becomes $3 \lesssim \mathrm{Pe} \lesssim 10$. Comparing to typical values reported in the experimental literature [38], we find that this condition can be easily reached for a wide range of microswimmers.

Physical mechanism.—We now provide a physical interpretation of the phenomenon, which elucidates qualitatively the mechanism at the origin of ANM. At low density of bath particles, the obstacles can be assumed to diffuse independently. For a given orientation of the active force χ, the average waiting time of the tracer between two jumps is $\tau + \rho\tau_p^{(\chi)}$, where $\tau_p^{(\chi)}$ is the mean time that the tracer spends with a bath particles on one of its neighboring sites and accounts for the "trapping" effect caused by the passive crowders. We can evaluate this typical time by considering that, when the tracer is at a given site $\boldsymbol{R}$ and is blocked by a crowder located at site $\boldsymbol{R} + \boldsymbol{e}_1$, the tracer can move forward if one of these three independent events, which follow exponential laws, takes place: (i) the obstacle moves in a transverse direction with characteristic time $2d\tau^*/(2d-2)$; (ii) the active force changes direction with characteristic time τ_α; and (iii) the tracer moves in a direction transverse to the direction of the obstacle with characteristic time $\tau/(1 - p_1^{(\chi)} - p_{-1}^{(\chi)})$. The mean trapping time therefore follows an exponential law of characteristic time $\tau_p^{(\chi)}$ given by

$$\frac{1}{\tau_p^{(\chi)}} = \frac{(2d-2)}{2d\tau^*} + \frac{1}{\tau_\alpha} + \frac{(1 - p_1^{(\chi)} - p_{-1}^{(\chi)})}{\tau}. \tag{6}$$

The velocity of the tracer is then estimated as an average over the directions of active force χ,

$$V \simeq \frac{1}{2d}\sum_\chi \frac{p_1^{(\chi)} - p_{-1}^{(\chi)}}{\tau + \rho\tau_p^{(\chi)}}, \tag{7}$$

and the condition for the existence of absolute negative mobility is given by $dV/dF_E|_{F_E=0} < 0$. Using the estimate of $\tau_p^{(\chi)}$ given by Eq. (6), we plot the critical value of the average jump time of the bath particles τ_c^* above which ANM is expected as a function of the active force F_A (Fig. 3), for different values of τ_α. This is compared to the result from the decoupling approximation, and it appears that our simple low-density argument is valid in a very wide range of parameters.

These physical considerations show how, in the low-density limit, the trapping of the tracer by passive crowders can result in ANM when its activity is strong enough. However, we emphasize that this approach would fail in dense regimes, where the correlations between the passive crowders would become predominant and would come into play. Moreover, the nontrivial response of the environment to the displacement of the tracer when ANM occurs [Fig. 2(b)] cannot be predicted within this simplified framework. The complete analytical solution presented above, which stems from the master equation, and which correctly captures these effects, is therefore necessary to fully describe the present problem. Finally, note that, in the case of an active tracer without external force, these trapping effects were also at the origin of the nonmonotonicity of its diffusion coefficient as a function of the persistence time τ_α [36]. Even though this did not involve the same parameters as ANM, it shows how the two effects are actually interlinked.

Conclusion.—We have shown that ANM can be observed in a minimal model for an active particle submitted to a constant external force as a result of its interactions with the other particles in its environment. The analytical treatment of our microscopic theory provides an expression of the velocity of the tracer in this setting, allows us to determine the conditions for ANM to be observed, and gives insight into the response of the environment to the nonequilibrium dynamics of the tracer. Our framework can be applied to more complex geometries (channel-like systems, for instance), and open new theoretical challenges: first, it will be interesting to investigate how the present conclusions can be extended to continuous-space situations, which will require other numerical and analytical techniques; second, the behavior of an active, driven tracer in a very dense bath of crowders will be of particular interest, as many active matter theories are now well explored in the high-density regime [39,40].

A. S. warmly thanks Ralph Eichhorn for fruitful discussions, in particular, on the qualitative argument for ANM. A. S. acknowledges partial support from MUR (Italian Ministry of University and Research) Project No. PRIN201798CZLJ.

[1] R. Kubo, The fluctuation-dissipation theorem, Rep. Prog. Phys. **29**, 255 (1966).

[2] U. M. B. Marconi, A. Puglisi, L. Rondoni, and A. Vulpiani, Fluctuation-dissipation: Response theory in statistical physics, Phys. Rep. **461**, 111 (2008).

[3] R. Eichhorn, P. Reimann, and P. Hänggi, Brownian Motion Exhibiting Absolute Negative Mobility, Phys. Rev. Lett. **88**, 190601 (2002).

[4] A. Ros, R. Eichhorn, J. Regtmeier, T. T. Duong, P. Reimann, and D. Anselmetti, Absolute negative particle mobility, Nature (London) **436**, 928 (2005).

[5] R. Eichhorn, J. Regtmeier, D. Anselmetti, and P. Reimann, Negative mobility and sorting of colloidal particles, Soft Matter **6**, 1858 (2010).

[6] J. Luo, K. A. Muratore, E. A. Arriaga, and A. Ros, Deterministic absolute negative mobility for micro- and submicrometer particles induced in a microfluidic device, Anal. Chem. **88**, 5920 (2016).

[7] A. Słapik, J. Łuczka, P. Hänggi, and J. Spiechowicz, Tunable Mass Separation via Negative Mobility, Phys. Rev. Lett. **122**, 070602 (2019).

[8] B. Cleuren and C. Van den Broeck, Random walks with absolute negative mobility, Phys. Rev. E **65**, 030101(R) (2002).

[9] M. Kostur, L. Machura, P. Hänggi, J. Łuczka, and P. Talkner, Forcing inertial Brownian motors: Efficiency and negative differential mobility, Physica (Amsterdam) **371A**, 20 (2006).

[10] L. Machura, M. Kostur, P. Talkner, J. Łuczka, and P. Hänggi, Absolute Negative Mobility Induced by Thermal Equilibrium Fluctuations, Phys. Rev. Lett. **98**, 040601 (2007).

[11] D. Speer, R. Eichhorn, and P. Reimann, Transient chaos induces anomalous transport properties of an underdamped Brownian particle, Phys. Rev. E **76**, 051110 (2007).

[12] J. Cividini, D. Mukamel, and H. Posch, Driven tracer with absolute negative mobility, J. Phys. A **51**, 085001 (2018).

[13] J. Wang, G. Casati, and G. Benenti, Inverse Currents in Hamiltonian Coupled Transport, Phys. Rev. Lett. **124**, 110607 (2020).

[14] A. Sarracino, F. Cecconi, A. Puglisi, and A. Vulpiani, Nonlinear Response of Inertial Tracers in Steady Laminar Flows: Differential and Absolute Negative Mobility, Phys. Rev. Lett. **117**, 174501 (2016).

[15] F. Cecconi, A. Puglisi, A. Sarracino, and A. Vulpiani, Anomalous force-velocity relation of driven inertial tracers in steady laminar flows, Eur. Phys. J. E **40**, 81 (2017).

[16] B.-q. Ai, W.-j. Zhu, Y.-f. He, and W.-r. Zhong, Giant negative mobility of inertial particles caused by the periodic potential in steady laminar flows, J. Chem. Phys. **149**, 164903 (2018).

[17] T. Chou, K. Mallick, and R. K. P. Zia, Non-equilibrium statistical mechanics: From a paradigmatic model to biological transport, Rep. Prog. Phys. **74**, 116601 (2011).

[18] K. Mallick, The exclusion process: A paradigm for non-equilibrium behaviour, Physica (Amsterdam) **418A**, 17 (2015).

[19] K. Nakazato and K. Kitahara, Site blocking effect in tracer diffusion on a lattice, Prog. Theor. Phys. **64**, 2261 (1980).

[20] K. W. Kehr, R. Kutner, and K. Binder, Diffusion in concentrated lattice gases. Self-diffusion of noninteracting particles in three-dimensional lattices, Phys. Rev. B **23**, 4931 (1981).

[21] R. A. Tahir-Kheli and R. J. Elliott, Correlated random walk in lattices: Tracer diffusion at general concentration, Phys. Rev. B **27**, 844 (1983).

[22] S. Leitmann and T. Franosch, Nonlinear Response in the Driven Lattice Lorentz Gas, Phys. Rev. Lett. **111**, 190603 (2013).

[23] S. Leitmann and T. Franosch, Time-Dependent Fluctuations and Superdiffusivity in the Driven Lattice Lorentz Gas, Phys. Rev. Lett. **118**, 018001 (2017).

[24] J. Cividini, D. Mukamel, and H. A. Posch, Driven tracers in narrow channels, Phys. Rev. E **95**, 012110 (2017).

[25] S. Pigeon, K. Fogelmark, B. Söderberg, G. Mukhopadhyay, and T. Ambjörnsson, Tracer particle diffusion in a system

with hardcore interacting particles, J. Stat. Mech. (2017) 123209.

[26] O. Benichou, P. Illien, G. Oshanin, A. Sarracino, and R. Voituriez, Tracer diffusion in crowded narrow channels. Topical review, J. Phys. Condens. Matter **30**, 443001 (2018).

[27] P. Baerts, U. Basu, C. Maes, and S. Safaverdi, Frenetic origin of negative differential response, Phys. Rev. E **88**, 052109 (2013).

[28] O. Bénichou, P. Illien, G. Oshanin, A. Sarracino, and R. Voituriez, Microscopic Theory for Negative Differential Mobility in Crowded Environments, Phys. Rev. Lett. **113**, 268002 (2014).

[29] M. Baiesi, A. L. Stella, and C. Vanderzande, Role of trapping and crowding as sources of negative differential mobility, Phys. Rev. E **92**, 042121 (2015).

[30] O. Bénichou, P. Illien, G. Oshanin, A. Sarracino, and R. Voituriez, Nonlinear response and emerging nonequilibrium micro-structures for biased diffusion in confined crowding environments, Phys. Rev. E **93**, 032128 (2016).

[31] C. Reichhardt and C. O. Reichhardt, Negative differential mobility and trapping in active matter systems, J. Phys. Condens. Matter **30**, 015404 (2017).

[32] R. Zia, E. Praestgaard, and O. Mouritsen, Getting more from pushing less: Negative specific heat and conductivity in nonequilibrium steady states, Am. J. Phys. **70**, 384 (2002).

[33] C. Maes, *Non-Dissipative Effects in Nonequilibrium Systems* (Springer, New York, 2017).

[34] See Supplemental Material at http://link.aps.org/supplemental/10.1103/PhysRevLett.130.218201 for details on numerical simulations and analytical calculations.

[35] P. Illien, O. Bénichou, G. Oshanin, A. Sarracino, and R. Voituriez, Nonequilibrium Fluctuations and Enhanced Diffusion of a Driven Particle in a Dense Environment, Phys. Rev. Lett. **120**, 200606 (2018).

[36] P. Rizkallah, A. Sarracino, O. Bénichou, and P. Illien, Microscopic Theory for the Diffusion of an Active Particle in a Crowded Environment, Phys. Rev. Lett. **128**, 038001 (2022).

[37] M. Baiesi, C. Maes, and B. Wynants, The modified Sutherland-Einstein relation for diffusive non-equilibria, Proc. R. Soc. A **467**, 2792 (2011).

[38] C. Bechinger, R. Di Leonardo, H. Löwen, C. Reichhardt, G. Volpe, and G. Volpe, Active Brownian particles in complex and crowded environments, Rev. Mod. Phys. **88**, 045006 (2016).

[39] L. Caprini, Umberto Marini Bettolo Marconi, C. Maggi, M. Paoluzzi, and A. Puglisi, Hidden velocity ordering in dense suspensions of self-propelled disks, Phys. Rev. Res. **2**, 023321 (2020).

[40] G. Szamel and E. Flenner, Long-ranged velocity correlations in dense systems of self-propelled particles, Europhys. Lett. **133**, 60002 (2021).